Spectral butterfly and electronic localization in rippled-graphene nanoribbons: Mapping onto effective one-dimensional chains

Pedro Roman-Taboada[1,*] and Gerardo G. Naumis[2,†]

[1]*Departamento de Física-Química, Instituto de Física, Universidad Nacional Autónoma de México (UNAM),
Apartado Postal 20-364, 01000 México, Distrito Federal, Mexico*
[2]*School of Physics, Astronomy and Computational Sciences, George Mason University, Fairfax, Virginia 22030, USA*

We report an exact map into one-dimensional effective chains of the tight-binding Hamiltonian for electrons in armchair and zigzag graphene nanoribbons with any uniaxial ripple. This mapping is used for studying the effect of uniaxial periodic ripples, taking into account the relative orientation changes between π orbitals. Such effects are important for short-wavelength ripples, while for long-wave ones, the system behaves nearly as strained graphene. The spectrum has a complex nature, akin to the Hofstadter butterfly with a rich localization behavior. Gaps at the Fermi level and dispersionless bands were observed, as well. The complex features of the spectrum arise as a consequence of the quasiperiodic or periodic nature of the effective one-dimensional system. Some features of these systems can be understood by considering weakly coupled dimers. The eigenenergies of such dimers are highly degenerate, and the net effect of the ripple can be seen as a perturbation potential that splits the energy spectrum. Several particular cases were analytically solved to understand this feature.

I. INTRODUCTION

Graphene, which is a two-dimensional (2D) crystal made from carbon, has incredible electronic, optical, and mechanical properties [1,2]. However, it is very difficult to grow perfectly flat graphene [3–6]. Instead, graphene presents corrugations and ripples that can improve or diminish its electronic conductivity [7–10]. Hence, the understanding of how corrugations and ripples modify the electronic properties of graphene is a very important issue. Furthermore, such knowledge can provide a way to tailor the electronic properties of graphene via mechanical deformation [11–13]. Even though the uniform and homogeneous strain has reached a level of good understanding [7,14,15], out-of-plane deformation effects are not well understood. Moreover, most of the available theories are limited to the case of low energies or long wavelengths, in which it is possible to write an effective Dirac equation with effective pseudomagnetic fields [16–18].

In a recent set of papers, we have shown that this picture can be modified for shorter wavelengths since a quasiperiodic fractal behavior, nontreatable under perturbation theory, can appear [19,20]. At the same time, an experimental observation of the effect has recently been made [21]. This behavior is not new in graphene; actually, this fractality has been extensively studied in graphene under magnetic fields within the Dirac approach [22–25]. However, a study of this behavior as a consequence of strain or corrugation using a tight-binding approach does not appear to have been made. The aim of this work is to understand how ripples modify the electronic properties of armchair (AGNs) and zigzag (ZGNs) graphene nanoribbons. To get such understanding, here we propose the study of uniaxial ripples using a tight-binding Hamiltonian.

Uniaxial ripples already show the expected effects in more general cases, and at the same time, it is possible to map the system into one-dimensional (1D) chains. This procedure is similar to that used for studying electrons in lattices under magnetic fields, in which it is possible to obtain the spectrum by studying the one-dimensional Harper equation [26,27]. Once this connection is established, we propose the study of the physical effects using uniaxial periodic ripples. As we will see, the energy spectrum has a fractal structure with gaps at the Fermi level. This highlights the importance of the rational or irrational nature of the ripple's wavelength. Furthermore, we are able to solve several cases analytically, leading to expressions for the bands as a function of the ripple's parameters: wavelength and amplitude.

The layout of this work is the following: In Sec. II, we discuss the details of mapping AGNs and ZGNs under any uniaxial ripple into effective 1D chains. In Sec. III, we study a particular case, a uniaxial periodic ripple, using the previous maps. The properties of the energy spectrum as a function of the frequency of the ripple, the band structure, and the density of states (DOS) are discussed, as well. Finally, in Sec. IV, our conclusions are presented.

II. MAPPING OF UNIAXIAL RIPPLED GRAPHENE INTO AN EFFECTIVE ONE-DIMENSIONAL SYSTEM

In this section, we will show how to reduce the study of uniaxial ripples in graphene to an effective one-dimensional system. We start with a graphene nanoribbon, as shown in Figs. 1 and 2, with a uniaxial deformation in the y direction due to a ripple in the graphene sheet. The new positions of carbon atoms in the rippled graphene are

$$\boldsymbol{r}' = (\boldsymbol{r}, z(\boldsymbol{r})), \tag{1}$$

where $\boldsymbol{r} = (x, y, 0)$ are the unrippled coordinates of carbon atoms, and $z(\boldsymbol{r})$ is the height variable in terms of the position $\boldsymbol{r}$. To obtain the electronic properties, we use a one-orbital next-nearest-neighbor tight-binding Hamiltonian in a honeycomb

---

*peter89@fisica.unam.mx
†On sabbatical leave from Departamento de Física-Química, Instituto de Física, Universidad Nacional Autónoma de México (UNAM), Apartado Postal 20-364, 01000 México, Distrito Federal, Mexico.
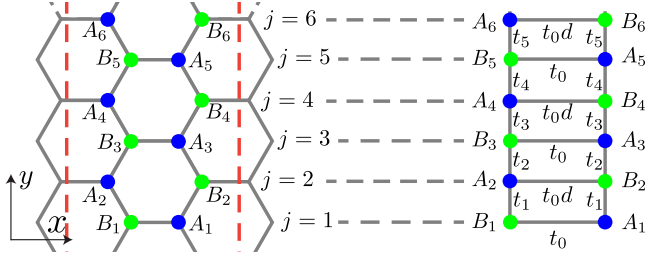
FIG. 1. (Color online) Primitive cell for AGNs (on the left between the red dotted lines) which is made for $2N$ atoms, i.e., N atoms of type A (blue solid circles) and N atoms of type B (green solid circles), we order the basis as $A_1, B_2, \ldots, B_{N-1}, A_N, B_1, A_2, \ldots, B_{N-1}, B_N$. We vary the height of each atom along the y direction. For this case the hopping parameter just depends upon the y component of the in-plane atom positions. The system is equivalent to the one-dimensional effective ladder shown at the right, where the label j corresponds to each ladder step in the y direction, t_j is the hopping integral for hopping from the atom A_j (B_j) to the atom B_{j+1} (A_{j+1}), and d is a coefficient that depends upon the momentum k_x.

lattice, given by [28]

$$H = -\sum_{\boldsymbol{r}',n} t_{\boldsymbol{r}',\boldsymbol{r}'+\boldsymbol{\delta}'_n} c^{\dagger}_{\boldsymbol{r}'} c_{\boldsymbol{r}'+\boldsymbol{\delta}'_n} + \text{H.c.}, \tag{2}$$

where the sum over $\boldsymbol{r}'$ is taken for all sites of the deformed lattice. The vectors $\boldsymbol{\delta}'_n$ point to the three next-nearest neighbors of $\boldsymbol{r}'$. For unstrained graphene $\boldsymbol{\delta}'_n = \boldsymbol{\delta}_n$ where

$$\boldsymbol{\delta}_1 = \frac{a}{2}(1, -\sqrt{3}, 0), \quad \boldsymbol{\delta}_2 = \frac{a}{2}(1, \sqrt{3}, 0), \quad \boldsymbol{\delta}_3 = a(-1, 0, 0), \tag{3}$$

and $c^{\dagger}_{\boldsymbol{r}'}$ and $c_{\boldsymbol{r}'}$ are the creation and annihilation operators of an electron at the lattice position $\boldsymbol{r}'$. In this model, the hopping integral $t_{\boldsymbol{r}',\boldsymbol{r}'+\boldsymbol{\delta}'_n}$ depends upon the strain, since the overlap between graphene orbitals is modified as the interatomic distances change. When corrugation is present, the π orbitals are no longer parallel. Let us denote by $\theta_{\boldsymbol{r}'}$ the angle which determines the relative orientation of a carbon atom in the
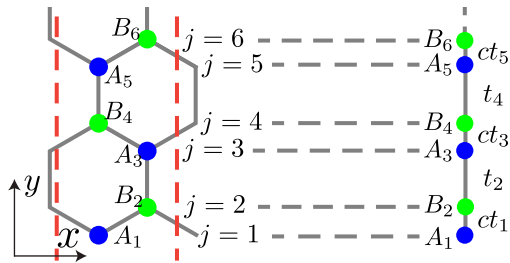

FIG. 2. (Color online) Primitive cell for ZGNs (to the left, delimited by two red dotted lines) made of N atoms ($N/2$ atoms of type A and $N/2$ atoms of type B). The basis is ordered as $A_1, B_2, \ldots, A_{N-1}, B_N$. The height z of every atom is modified only in the y direction. Then the hopping parameter is no longer constant but depends upon the y component of the atom's positions. This system can be mapped into a one-dimensional effective chain (on the left) where j labels the site along the zigzag direction, t_j is the hopping parameter for hopping from the jth atom to the $(j+1)$th atom, and c is a coefficient that depends on the momentum in the x direction.

position $\boldsymbol{r}'$ in the graphene nanoribbon. This angle depends on the local curvature of the layer. The effect of the relative orientation change of the π orbitals and the interatomic distance changes are described by [29–31]

$$t_{\boldsymbol{r}',\boldsymbol{r}'+\boldsymbol{\delta}'_n} = t_0 \big[1 + \alpha \big(1 - \boldsymbol{N}_{\boldsymbol{r}'} \cdot \boldsymbol{N}_{\boldsymbol{r}'+\boldsymbol{\delta}'_n} \big) \big]$$
$$\times \exp \big[-\beta(l_{\boldsymbol{r}',\boldsymbol{r}'+\boldsymbol{\delta}'_n}/a - 1) \big], \tag{4}$$

where $\boldsymbol{N}_{\boldsymbol{r}'}$ is the unit vector normal to the surface at the site $\boldsymbol{r}'$, given by

$$\boldsymbol{N}_{\boldsymbol{r}'} = \frac{\hat{\boldsymbol{z}} - \nabla z}{\sqrt{1 + (\nabla z)^2}}, \tag{5}$$

and $\nabla = (\partial_x, \partial_y)$ is the 2D gradient operator while $\hat{\boldsymbol{z}}$ is the unit vector in the direction perpendicular to the plane. $l_{\boldsymbol{r}',\boldsymbol{r}'+\boldsymbol{\delta}'_n}$ is the interatomic distance between two neighbor sites after a ripple is applied, and $\alpha \approx 0.4$ is a constant that accounts for the change of the relative orientation of the π orbitals. Here $\beta \approx 3.37$, and $t_0 \approx 2.7$ eV corresponds to graphene without strain. The unrippled bond length is denoted by a. For the purpose of this paper, it is natural to measure the distances in units of a, which is equivalent to setting $a = 1$. In other words, all the distances and lengths will be measured in units of a. It is important to remark that contributions from terms containing β are due to distance changes, while terms dependent on α account for angular changes of the orbital overlap. As we will see, β-dependent terms tend to shrink the energy spectrum whereas α-dependent terms tend to stretch it.

Now, for a uniaxial ripple the interatomic distances between carbon atoms can be written as

$$l_{\boldsymbol{r}',\boldsymbol{r}'+\boldsymbol{\delta}'_n} = \big|\big| \boldsymbol{\delta}_n + \big[z\big(y + \delta_n^{(y)}\big) - z(y) \big] \hat{\boldsymbol{z}} \big|\big|$$
$$= \sqrt{1 + \big[z\big(y + \delta_n^{(y)}\big) - z(y) \big]^2}. \tag{6}$$

Recently, we have shown that is possible to map armchair and zigzag graphene nanoribbons under uniaxial strain onto an effective one-dimensional system [19,20]. In the next section, we extend these results for AGNs and ZGNs under uniaxial ripples.

Before entering the details of the maps and for comparison purposes with other works, it is important to remark that for small-amplitude and long-wavelength ripples, we have $(1 - \boldsymbol{N}_{\boldsymbol{r}'} \cdot \boldsymbol{N}_{\boldsymbol{r}'+\boldsymbol{\delta}'_n}) \approx \theta^2_{\boldsymbol{r}',\boldsymbol{r}'+\boldsymbol{\delta}'_n}/2$, where $\theta_{\boldsymbol{r}',\boldsymbol{r}'+\boldsymbol{\delta}'_n}$ is the angle between π orbitals at the sites $\boldsymbol{r}'$ and $\boldsymbol{r}' + \boldsymbol{\delta}'_n$. In such a case, since $\alpha < \beta$ and the angle correction is quadratic, it follows that

$$t_{\boldsymbol{r}',\boldsymbol{r}'+\boldsymbol{\delta}'_n} \approx t_0 \Big[1 + \frac{\alpha}{2} \theta^2_{\boldsymbol{r}',\boldsymbol{r}'+\boldsymbol{\delta}'_n} \Big] \exp \big[-\beta(l_{\boldsymbol{r}',\boldsymbol{r}'+\boldsymbol{\delta}'_n} - 1) \big]$$
$$\approx t_0 \big[1 - \beta \big(l_{\boldsymbol{r}',\boldsymbol{r}'+\boldsymbol{\delta}'_n} - 1 \big) \big]. \tag{7}$$

In this limit, the model resembles graphene nanoribbons under planar strain. As we will show, our general computations are consistent with this limit, providing a test for the method presented here.

A. Armchair graphene nanoribbon

When a uniaxial ripple in the y direction is applied, it is possible to describe the electronic properties of the AGN by an effective one-dimensional Hamiltonian. We start by labeling

the atom's positions as shown in Fig. 1, i.e., we order the basis as $A_1, B_2, A_3, \ldots, A_{N-1}, B_N$ and $B_1, A_2, B_3, \ldots, A_{N-1}, B_N$. Thus, the effective one-dimensional Hamiltonian can be written as [20]

$$H_{\text{AGN}}(k_x) = \sum_j t_0 [d(k_x) a_{2j}^\dagger b_{2j} + a_{2j+1}^\dagger b_{2j+1}]$$
$$+ \sum_j t_j^{\text{AGN}} a_j^\dagger b_{j+1} + \text{H.c.}, \qquad (8)$$

where $d(k_x) = \exp(ik_x)$, $a_j, a_j^\dagger$, and $b_j, b_j^\dagger$ are the annihilation and creation operators in the sublattices A and B in graphene, respectively. This effective Hamiltonian describes two modulated chains, as is shown in Fig. 1. t_j^{AGN} is the hopping parameter between the $j+1$ and j atoms in the y direction, given by

$$t_j^{\text{AGN}} = t_0 \big[1 + \alpha \big(1 - \mathbf{N}_{j+1}^{\text{AGN}} \cdot \mathbf{N}_j^{\text{AGN}} \big) \big]$$
$$\times \exp \big[-\beta \big(l_{j+1,j}^{\text{AGN}} - 1 \big) \big], \qquad (9)$$

where

$$l_{j+1,j}^{\text{AGN}} = \sqrt{1 + \left[z\big(y_{j+1}^{\text{AGN}} \big) - z\big(y_j^{\text{AGN}} \big) \right]^2} \qquad (10)$$

is the interatomic distance between the atoms in sites $j+1$ and j,

$$y_j^{\text{AGN}} = y_A^{\text{AGN}}(j) = y_B^{\text{AGN}}(j) = \sqrt{3}(j-1)/2 \qquad (11)$$

are the positions for atoms A and B, and $j = 1, 2, \ldots, N$ labels the sites along the y direction for pristine graphene. Finally the unitary normal vector is $\mathbf{N}_j^{\text{AGN}} = \mathbf{N}(y_j^{\text{AGN}})$ defined as in Eq. (5).

B. Zigzag graphene nanoribbon

Similarly, when we apply a uniaxial ripple to a zigzag graphene nanoribbon, it is possible to map the system into a one-dimensional effective chain. If we label the basis as $A_1, B_2, \ldots, A_{N-1}, B_N$, as shown in Fig. 2, the resulting Hamiltonian is [19]

$$H_{\text{ZGN}}(k_x) = \sum_j \big[c(k_x) t_{2j+1}^{\text{ZGN}} a_{2j+1}^\dagger b_{2j+2} + t_{2j+2}^{\text{ZGN}} b_{2j+2} a_{2j+3}^\dagger \big]$$
$$+ \text{H.c.}, \qquad (12)$$

where $c(k_x) = 2\cos\sqrt{3}k_x/2$,

$$t_j^{\text{ZGN}} = t_0 \big[1 + \alpha \big(1 - \mathbf{N}_{j+1}^{\text{ZGN}} \cdot \mathbf{N}_j^{\text{ZGN}} \big) \big]$$
$$\times \exp \big[-\beta \big(l_{j+1,j}^{\text{ZGN}} - 1 \big) \big] \qquad (13)$$

is the hopping parameter between the sites $j+1$ and j in the y direction, $\mathbf{N}_j^{\text{ZGN}} = \mathbf{N}(y_j^{\text{ZGN}})$ defined as in Eq. (5), and

$$l_{j+1,j}^{\text{ZGN}} = \sqrt{1 + \left[z\big(y_{j+1}^{\text{ZGN}} \big) - z\big(y_j^{\text{ZGN}} \big) \right]^2}, \qquad (14)$$

where

$$y_j^{\text{ZGN}} = y^{\text{ZGN}}(j) = \frac{1}{4}\big\{ 3j + \frac{1}{2}[1 - (-1)^j] \big\} \qquad (15)$$

are the positions of carbon atoms in unrippled graphene and $j = 1, 2, \ldots, N$ labels the sites as is displayed in Fig. 2.

III. UNIAXIAL PERIODIC RIPPLE

Let us now study in this section the particular case of a periodic uniaxial ripple. This kind of corrugation is commonly observed when graphene is grown on a substrate [6]. In particular, we will consider that the periodic uniaxial ripple has the following form:

$$z(y) = \lambda \cos(2\pi\sigma y + \phi). \qquad (16)$$

This particular oscillation contains three parameters: wavelength (controlled by the parameter σ), amplitude (controlled by λ), and phase (controlled by ϕ). Thus, σ is translated into a ripple with a spatial wavelength Λ such that $\Lambda = 2\pi a/\sigma$. Small σ's compared with the lattice parameter a are translated into long-wavelength ripples. The amplitude λ is the maximal height reached by the ripples, usually given in nanometers or in percentages of a.

Now we wil discuss briefly the feasibility of such a specific ripple. Since graphene exhibits a high asymmetry in tensile versus compressive strain, i.e., while the C-C bond length can be tensile up to 25% [2] of the lattice parameter, it is almost incompressible because this would induce out-of-plane deformations. Thus, in general, to produce this ripple it is enough to apply uniaxial strain. Also, it has been observed that, growing graphene on a substrate, 1D periodic graphene ripples can be built by using thermal strain engineering and the anisotropic stress due to the substrate [32]. On the other hand, as we will see later, we will use a big ripple's amplitude ($\lambda = 80\%$ of the lattice parameter) in all of our plots for illustrative proposes. Even though this value is high, the most important of our results depend only upon the ripple's wavelength (σ) and are valid for all values of λ.

Another important aspect of the electronic properties is the wave function localization. For studying it, we will use the normalized participation ratio (N_{PR}), defined as

$$N_{\text{PR}}(E) = \frac{\ln \sum_{j=1}^N |\psi(j)|^4}{\ln N}. \qquad (17)$$

This quantity is a measure of the wavefunction localization [33] for extended states $N_{\text{PR}} \to -1$ (blue color in the figures), whereas it tends to zero for localized states (red color in the figures). In the next section, we will study the physical effects on the electronic properties of AGNs and ZGNs under the previously described periodic ripples.

A. AGNs with uniaxial periodic ripples

When we apply a uniaxial periodic ripple as given by Eq. (16) to AGNs, the hopping integral becomes

$$t_j^{\text{AGN}} = t_0 \big[1 + \alpha \big(1 - \mathbf{N}_{j+1}^{\text{AGN}} \cdot \mathbf{N}_j^{\text{AGN}} \big) \big]$$
$$\times \exp \left\{ -\beta \left[\sqrt{1 + 4\lambda^2 \sin^2\left(\frac{\sqrt{3}}{2}\pi\sigma\right) \xi_A^2(j+1/2)} - 1 \right] \right\},$$
$$(18)$$

where $\xi_A(j) = \sin(\sqrt{3}\pi\sigma j + \phi)$. To get a better understanding, it is worth considering the small-amplitude case. Using
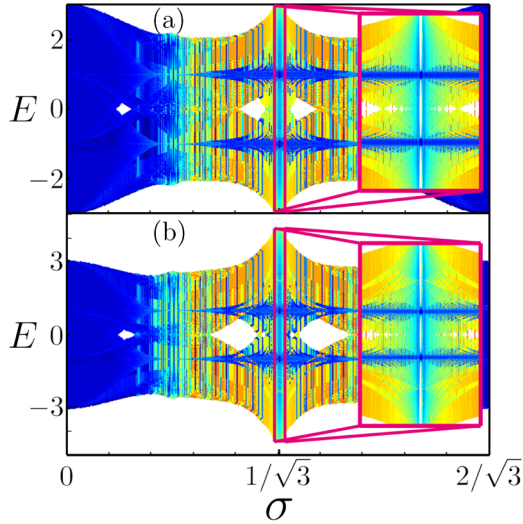
FIG. 3. (Color online) Energy spectrum of AGNs as a function of σ for $\lambda = 0.8$, using (a) $\alpha = 0.4$ and (b) $\alpha = 0$ obtained by solving the Schrödinger equation for a system of 400 atoms, using 250 grid points for sampling k_x and with cyclic boundary conditions. The different colors represent the normalized participation ratio $N_{PR}(E)$.

Eq. (18), the hopping interchain parameter becomes

$$t_j^{AGN} \approx t_0 \exp\left[-2\beta\lambda^2 \sin^2\left(\frac{\sqrt{3}}{2}\pi\sigma\right)\xi^2(j+1/2)\right]$$

$$\approx t_0 - 2t_0\beta\lambda^2 \sin^2\left(\frac{\sqrt{3}}{2}\pi\sigma\right)\xi^2(j+1/2). \quad (19)$$

This expression is quite similar to the hopping integral that appears in the off-diagonal Harper model [26]; the main difference here is that all terms are squared. Hence, we expect the period in σ to be half of the period of AGNs under uniaxial periodic strain. Otherwise, both spectra would be really similar in the low-energy or long-wavelength limit, as can be confirmed in Fig. 3. Therein, it is shown the spectrum of H_{AGN} as a function of σ for (a) $\alpha = 0$ and (b) $\alpha = 0.4$, obtained using cyclic boundary conditions by diagonalizing the resulting matrix for each value of k_x. Many interesting features are observed. First, the spectrum has a fractal nature with gaps at the Fermi level. Second, we observe that localized states coexist with extended ones. It is easy to understand this feature, since when the period of the lattice is commensurable with the ripple's period the system behaves as a modulated crystal, and the states have a Bloch nature; these are extended. When the periods are incommensurate with each other, the system behaves as a quasicrystal and the wave functions tend to have different localization properties. Finally, we observe that the effect of relative orientation changes between π orbitals (i.e., the α-dependent-term effects) is to produce a widening of the spectrum, which becomes important for σ around $1/\sqrt{3}$. To gain further insight into the spectrum, consider the interesting transition seen as σ goes from zero to $\sigma = 1/\sqrt{3}$, as shown in detail in Fig. 4. Therein, the band structure is displayed for (a) $\sigma = 0.6/\sqrt{3}$, (b) $\sigma = 0.8/\sqrt{3}$, and (c) $\sigma = 1/\sqrt{3}$. This transition goes from unrippled graphene to a system made up of weakly coupled dimers. The dimers are made from pairs of
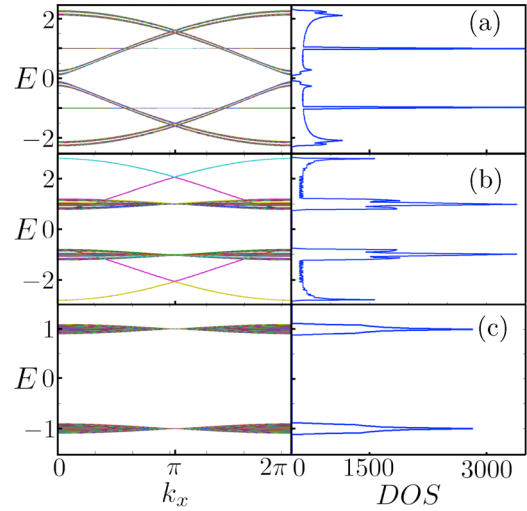

FIG. 4. (Color online) Band structure and density of states (DOS) of an AGN for $\phi = 0$ and $\lambda = 0.8$ using (a) $\sigma = 0.6/\sqrt{3}$, (b) $\sigma = 0.8/\sqrt{3}$, and (c) $\sigma = 1/\sqrt{3}$ for a system with 200 atoms. Cyclic boundary conditions were used.

sites joined by a horizontal bond as shown in Fig. 1. The dimers appear since for $\sigma = 1/\sqrt{3}$, the hopping parameter becomes $t_j^{AGN} = t(\lambda = 0.8) \approx 0.05t_0$. The exact expression of $t(\lambda)$ will be given in the next section. Thus, $t(\lambda = 0.8) \ll t_0$ and t_j can be considered as a weak perturbation to a system made of pure dimers. The eigenenergies of the dimers are highly degenerate, with values $E = \pm t_0$ as observed in Fig. 4(a). The effect of $t(\lambda)$ is just a widening around these values, giving a spectrum in the intervals $[\pm t_0 - t(\lambda = 0.8), \pm t_0 + t(\lambda = 0.8)]$, as observed in Fig. 4(a). As $\sigma \to 0$, the dimers evolve into the Van Hove singularity at $E = \pm t_0$ observed in unrippled graphene. Also, the system can be treated as a ladder with $t_j^{AGN} = \langle t \rangle + \delta_j$, where $\langle t \rangle$ is the average hopping parameter, and δ_j is a small perturbing potential, $\delta_j \ll \langle t \rangle$. For example, the case (c) in Fig. 4 corresponds to weakly coupled squares.

Before showing how the case $\sigma = 1/\sqrt{3}$ can be solved analytically, leading to weakly coupled dimers, let us discuss the band structures displayed in Fig. 5. Therein are shown the band structure and the DOS for σ values that are
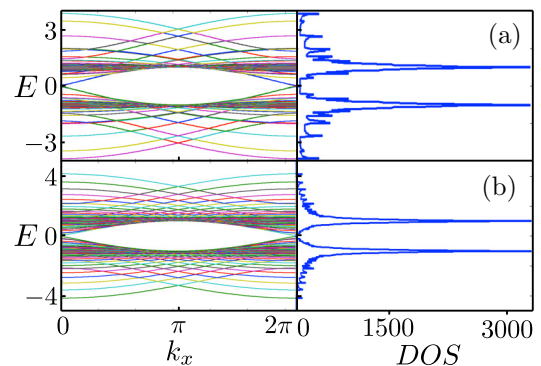

FIG. 5. (Color online) Band structure and DOS for an AGN using (a) $\sigma = 4\sqrt{5/3}$ and (b) $\sigma = 0.4\sqrt{7/3}$ for $\alpha = 0.4$ and the same conditions as in Fig. 4. Note that there are two partially flat bands at $E = \pm 1$ and that the DOS is spiky.

incommensurable with the period of unrippled AGNs. In these cases, the dimer model is still useful. When $t_j^{AGN} \rightarrow 0$ the effective system is made of dimers with two different intradimer hopping parameters t_0 and $t_0 d(k_x)$, with eigenenergies ± 1. These energies are highly degenerate because of the factor $d(k_x)$. When t_j^{AGN} becomes quasiperiodic, the degeneracy is broken and the spectrum is fragmented, as observed in Fig. 5. However, the other dimers with hopping parameter given by t_0 are not affected. This kind of dimers are the ones responsible for the partly flat bands at $\pm t_0$.

Particular case $\sigma = 1/\sqrt{3}$

For $\sigma = 1/\sqrt{3}$, the eigenergies can be calculated exactly. At this particular σ value the hopping integral can be written as follows:

$$t_j^{AGN} = t(\lambda) = t_0 \exp[-\beta(\sqrt{1 + 4\lambda^2} - 1)]. \quad (20)$$

Hence, the unit cell contains only four different kinds of site. Note that for big λ we have $t(\lambda) \rightarrow 0$ and the effective system is made of two different dimers, corresponding to horizontal pairs of atoms, with interdimer hopping parameter t_0 and $t_0 d(k_x)$. This confirms the previous discussion and the band structure shown in Fig. 4(c). The eigenenergies for such a system are

$$E(k_x) = \pm t_0 \sqrt{1 + [t(\lambda)]^2 \pm 2t(\lambda)|\cos(k_x/2)|}. \quad (21)$$

From the previous equation one can prove that the gap's size is

$$\Delta_{AGN} = 2|t(\lambda) - t_0|. \quad (22)$$

which is the same that we obtained using the intervals $[\pm t_0 - t(\lambda = 0.8), \pm t_0 + t(\lambda = 0.8)]$ when perturbation theory was applied. It is worth finding the minimum value of λ for opening a gap. It is easy to show that this occurs for any $\lambda > 0$, which is an important result for applications, due to the fact that it is possible to tailor the gap's size at the Fermi level by using Eq. (22) with a ripple amplitude within the elastic response of graphene.

B. ZGN with periodic uniaxial ripples

When a ripple given by Eq. (16) is applied to ZGNs, the hopping integral becomes

$$t_j^{AGN}$$
$$= t_0[1 + \alpha(1 - N_{j+1}^{ZGN} \cdot N_j^{ZGN})]$$
$$\times \exp\left\{-\beta\left[\sqrt{1 + 4\lambda^2 \sin^2\left(\frac{\pi}{2}\sigma\varphi_j\right)\xi_Z^2(3j/2 + 1)} - 1\right]\right\}, \quad (23)$$

where $\varphi_j = [3 + (-1)^j]/4$ and $\xi_Z(j) = \sin(\pi\sigma j + \phi)$. Further insight can be obtained by analyzing the case of small-amplitude ripples, in which the hopping parameter is as follows:

$$t_j^{ZGN} t_0 \approx \exp\left\{-2\beta\lambda^2 \sin^2\left(\frac{\pi}{2}\sigma\varphi_j\right)\xi_Z^2(3j/2 + 1)\right\}$$
$$\approx t_0 - 2t_0\beta\lambda^2 \sin^2\left(\frac{\pi}{2}\sigma\varphi_j\right)\xi_Z^2(3j/2 + 1). \quad (24)$$
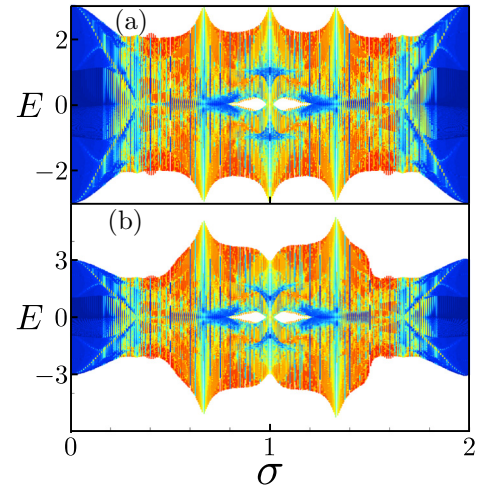

FIG. 6. (Color online) Energy spectrum of a ZGN as a function of σ for (a) $\lambda = 0.8$ and $\alpha = 0$, and (b) $\lambda = 0.8$ and $\alpha = 0.4$ obtained by solving the Schrödinger equation for a system of 80 atoms, using 250 grid points for sampling k_x and with cyclic boundary conditions. The different colors represent the normalized participation ratio $N_{PR}(E)$. Note that the gaps at the Fermi level are fewer and smaller than in AGN ripples; the wave functions are more localized as well.

Again, this hopping integral is very similar to that for ZGNs under uniaxial periodic strain [19]. As in AGNs, the main difference is that all terms are squared. That makes the period one-half of that in the uniaxially periodiclly strained ZGNs, as confirmed in Fig. 6. There in, we show the energy spectrum for ZGNs obtained using cyclic boundary conditions and by diagonalizing the corresponding matrix for each value of k_x. Two different values of α were used, (a) $\alpha = 0$ and (b) $\alpha = 0.4$. There are many interesting features. First, the states are more localized than in the AGN case. Second, the gaps at the Fermi level are smaller than the gaps in AGNs. Third, ZGNs are more sensitive to the effect of α; however, as in AGNs, this effect is just a widening of the energy spectrum. The structure still being the same as in the case $\alpha = 0$, especially for values near or at $\sigma = 2/3, 4/3$ [see Figs. 6(a) and 6(b)]. For $\sigma = 2/3, 4/3$, we have

$$t_j^{ZGN} = t_{eff}(\lambda) = t(3\lambda/4)\left[1 + \alpha\left(1 - \frac{1}{\sqrt{1 + 4\pi^2\lambda^2/3}}\right)\right], \quad (25)$$

where $t(\lambda)$ is given by Eq. (20). This equation does not depend upon the site. Substituting all the parameters and by using $\lambda = 0.8$, the hopping parameter is found to be $t_{eff}(\lambda = 0.8) \approx 0.19t_0$ for $\alpha = 0.4$ and $t_{eff}(\lambda = 0.8) \approx 0.15t_0$ for $\alpha = 0$. Thus, in these cases, the system has a ZGN-like spectrum with hopping parameter t_{eff}. Although t_{eff} depends upon α, this effect is small and the spectrum at the points $\sigma = 2/3, 4/3$ is very narrow, as seen in Fig. 6. For σ near to that point the spectrum is highly fragmented, because the α-dependent terms become important. They act as a perturbation potential, splitting the band structure; therefore, the spectrum is wider near $\sigma = 2/3, 4/3$, as can be observed in Fig. 7(b).

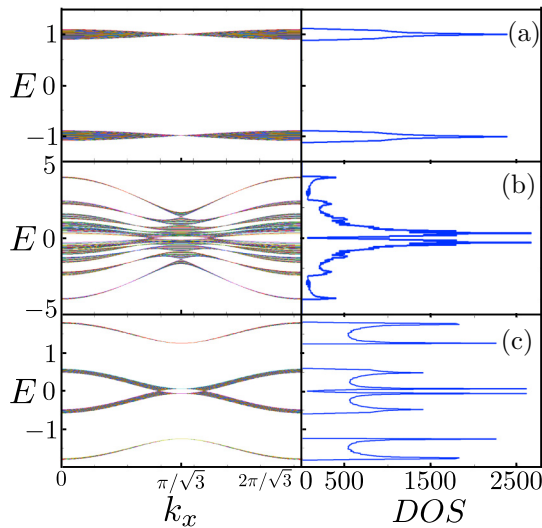Let us now discuss the transition observed in Fig. 7 as σ goes from zero to 1.

FIG. 7. (Color online) Band structure and density of states (DOS) of a ZGN for $\phi = 0$, $\lambda = 0.8$ using (a) $\sigma = 1$, (b) $\sigma = (\sqrt{5} - 1)/2$, and (c) $\sigma = 1/4$. The same conditions as in Fig. 6 were used. Note the big gap opened at the Fermi level in (a); in (b) the band structure is fragmented and hence the DOS has a lot of spikes, and in (c) the DOS is similar to that of linear chains weakly interacting.

1. Case $\sigma = 1/4$

For $\sigma = 1/4$, the band structure and DOS are shown in Fig. 7(c). In this case, the unit cell has only four different atoms, with hopping parameters given by

$$t_1^{\mathrm{ZGN}} = t_1 = t(\lambda/2)\left[1 + \alpha\left(1 - \frac{1}{\sqrt{1 + \pi^2\lambda^2}}\right)\right],$$

$$t_2^{\mathrm{ZGN}} = t_2 = t_0 + t_0\alpha\left(1 - \frac{1 - \pi^2\lambda^2}{1 + \pi^2\lambda^2}\right),$$

$$t_3^{\mathrm{ZGN}} = t_1,$$

$$t_4^{\mathrm{ZGN}} = t(\lambda),$$

where $t(\lambda)$ is defined in Eq. (20). The eigenenergies can be calculated exactly,

$$E(k_k) = \pm[t(\lambda) + t_2]$$
$$\pm\sqrt{[t(\lambda) - t_2]^2 + 16t_1^2\cos^2(\sqrt{3}k_x/2)}. \quad (27)$$

From the dispersion relation it can be seen that the system behaves as a linear chain with two different atoms, hopping parameter giving by t_1, and self-energies $t(\lambda)$ and t_2. When σ takes irrational values near $\sigma = 1/4$ the degeneracy is broken and the DOS becomes spiky, as can be seen in Fig. 7(b).

Finally, the case $\sigma = 1$ is displayed in Fig. 7. Note that this case [Fig. 7(a)] is the same as in Fig. 4(c). Let us explain this feature. When $\sigma = 1$, the hopping parameter takes two different values depending on the parity of j; if j is odd, $t_j^{\mathrm{ZGN}} = t_0$ whereas if it is even, $t_j^{\mathrm{ZGN}} = t(\lambda = 0.8) \approx 0.05t_0$. So the effective system is again made of dimers with intradimer hopping integrals given by $t(\lambda = 0.8)c(k_x)$ and t_0. Due to $t(\lambda = 0.8) \ll t_0$ the effective system can be seen as weakly coupled dimers with hopping parameter $t(\lambda = 0.8)c(k_x)$. Hence, the gap's size must be $2|2t(\lambda = 0.8) - t_0|$ the main

difference from AGNs is that here we have $2t(\lambda)$, due to $c(k_x) = 2\cos(\sqrt{3}k_x)/2$. This prediction will be confirmed by calculating the eigenenergies analytically in the next section.

2. Case $\sigma = 1$

We first calculate the hopping parameter

$$t_j^{\mathrm{ZGN}} = \begin{cases} t_0 & \text{if } j \text{ is even,} \\ t(\lambda) = \exp\{-\beta[\sqrt{1 + 4\lambda^2} - 1]\} & \text{if } j \text{ is odd.} \end{cases} \quad (28)$$

Thus, the effective system just has four different atoms per unit cell, and the effective chain is made of dimers with hopping parameter $t_0 c(k_x)$. The eigenenergies for this system as a function of λ and k_x are

$$E(k_x) = \pm t_0 \pm 2t(\lambda)\cos\left(\frac{\sqrt{3}}{2}k_x\right). \quad (29)$$

To confirm the gap's size predicted before, we calculate it from Eq. (29), resulting in

$$\Delta_{\mathrm{ZGN}} = 2|2t(\lambda) - t_0|. \quad (30)$$

In this case, a gap is opened for $\lambda \geqslant \lambda_C$, where

$$\lambda_C = \frac{1}{2}\sqrt{\left(1 + \frac{1}{\beta}\ln 2\right)^2 - 1} \approx 0.34. \quad (31)$$

This minimal value of λ_C for opening a gap at the Fermi level exceeds the elastic response of graphene and thus seems difficult to observe experimentally.

IV. CONCLUSIONS

Summarizing, we have analyzed the electronic properties of AGNs and ZGNs under uniaxial periodic ripples, using an exact mapping of the corresponding tight-binding Hamiltonian into effective one-dimensional chains. In particular, we studied uniaxial periodic ripples, finding complex spectra, gaps at the Fermi level, and flat bands for AGNs. All these features can be understood by looking at an effective system which is made of dimers. For instance, when σ is commensurable with the characteristic period of the lattice the effective system behaves as weakly coupled dimers resulting, for λ big, in flat bands for AGNs. However, when this is not the case, the reciprocal space becomes dense, which results in a fractal spectrum.

[1] K. S. Novoselov, A. K. Geim, S. V. Morozov, D. Jiang, Y. Zhang, S. V. Dubonos, I. V. Grigorieva, and A. A. Firsov, Science **306**, 666 (2004).

[2] C. Lee, X. Wei, J. W. Kysar, and J. Hone, Science **321**, 385 (2008).

[3] J. C. Meyer, A. K. Geim, M. I. Katsnelson, K. S. Novoselov, T. J. Booth, and S. Roth, Nature (London) **446**, 60 (2007).

[4] J. Meyer, A. Geim, M. Katsnelson, K. Novoselov, D. Obergfell, S. Roth, C. Girit, and A. Zettl, Solid State Commun. **143**, 101 (2007).

[5] E. Stolyarova, K. T. Rim, S. Ryu, J. Maultzsch, P. Kim, L. E. Brus, T. F. Heinz, M. S. Hybertsen, and G. W. Flynn, Proceedings of the National Academy of Sciences **104**, 9209 (2007).

[6] N. A. Vinogradov, A. A. Zakharov, V. Kocevski, J. Rusz, K. A. Simonov, O. Eriksson, A. Mikkelsen, E. Lundgren, A. S. Vinogradov, N. Mårtensson, and A. B. Preobrajenski, Phys. Rev. Lett. **109**, 026101 (2012).

[7] V. M. Pereira, A. H. Castro Neto, and N. M. R. Peres, Phys. Rev. B **80**, 045401 (2009).

[8] F. Guinea, in *Exploring Graphene, Recent Research Advances*, special issue of Solid State Commun. **152**, 1437 (2012).

[9] D. A. Bahamon and V. M. Pereira, Phys. Rev. B **88**, 195416 (2013).

[10] M. Oliva-Leyva and G. G. Naumis, J. Phys.: Condens. Matter **26**, 125302 (2014).

[11] V. M. Pereira and A. H. Castro Neto, Phys. Rev. Lett. **103**, 046801 (2009).

[12] M. T. Ong and E. J. Reed, ACS Nano **6**, 1387 (2012).

[13] D. Zhan, J. Yan, L. Lai, Z. Ni, L. Liu, and Z. Shen, Adv. Mater. **24**, 4055 (2012).

[14] E. Prada, P. San-Jose, G. León, M. M. Fogler, and F. Guinea, Phys. Rev. B **81**, 161402 (2010).

[15] M. Oliva-Leyva and G. G. Naumis, Phys. Rev. B **88**, 085430 (2013).

[16] M. M. Fogler, F. Guinea, and M. I. Katsnelson, Phys. Rev. Lett. **101**, 226804 (2008).

[17] D. A. Gradinar, M. Mucha-Kruczyński, H. Schomerus, and V. I. Fal'ko, Phys. Rev. Lett. **110**, 266801 (2013).

[18] R. Carrillo-Bastos, D. Faria, A. Latgé, F. Mireles, and N. Sandler, Phys. Rev. B **90**, 041411 (2014).

[19] G. G. Naumis and P. Roman-Taboada, Phys. Rev. B **89**, 241404 (2014).

[20] P. Roman-Taboada and G. G. Naumis, Phys. Rev. B **90**, 195435 (2014).

[21] C. R. Woods, L. Britnell, A. Eckmann, R. S. Ma, J. C. Lu, H. M. Guo, X. Lin, G. L. Yu, Y. Cao, R. V. Gorbachev, A. V. Kretinin, J. Park, L. A. Ponomarenko, M. I. Katsnelson, Y. Gornostyrev, K. Watanabe, T. Taniguchi, C. Casiraghi, H. J. Gao, A. K. Geim, and K. S. Novoselov, Nat. Phys. **10**, 451 (2014).

[22] N. Nemec and G. Cuniberti, Phys. Rev. B **75**, 201404 (2007).

[23] L. A. Chizhova, F. Libisch, and J. Burgdörfer, Phys. Rev. B **90**, 165404 (2014).

[24] G. Gumbs, A. Iurov, D. Huang, and L. Zhemchuzhna, Phys. Rev. B **89**, 241407 (2014).

[25] G. L. Yu, R. V. Gorbachev, J. S. Tu, A. V. Kretinin, Y. Cao, R. Jalil, F. Withers, L. A. Ponomarenko, B. A. Piot, M. Potemski, D. C. Elias, X. Chen, K. Watanabe, T. Taniguchi, I. V. Grigorieva, K. S. Novoselov, V. I. Fal'ko, A. K. Geim, and A. Mishchenko, Nat. Phys. **10**, 525 (2014).

[26] P. G. Harper, Proc. Phys. Soc., London, Sect. A **68**, 874 (1955).

[27] D. R. Hofstadter, Phys. Rev. B **14**, 2239 (1976).

[28] A. H. Castro Neto, F. Guinea, N. M. R. Peres, K. S. Novoselov, and A. K. Geim, Rev. Mod. Phys. **81**, 109 (2009).

[29] E.-A. Kim and A. H. C. Neto, EPL (Europhys. Lett.) **84**, 57007 (2008).

[30] R. M. Ribeiro, V. M. Pereira, N. M. R. Peres, P. R. Briddon, and A. H. C. Neto, New J. Phys. **11**, 115002 (2009).

[31] F. Guinea, M. I. Katsnelson, and A. K. Geim, Nat. Phys. **6**, 30 (2010).

[32] K.-K. Bai, Y. Zhou, H. Zheng, L. Meng, H. Peng, Z. Liu, J.-C. Nie, and L. He, Phys. Rev. Lett. **113**, 086102 (2014).

[33] G. G. Naumis, Phys. Rev. B **76**, 153403 (2007).